Impact Of Bundle Deformation On CHF: ASSERT-PV Assessment Of Extended Burnup Bruce B Bundle G85159W

Y.F. Rao* And A.M. Manzer**

* Atomic Energy of Canada Limited
Chalk River Laboratories
Chalk River, Canada K0J 1J0

**CANTECH Associates Ltd
Burlington, Canada
(formerly of AECL Sheridan Park)

This paper presents a subchannel thermalhydraulic analysis of the effect on critical heat flux (CHF) of bundle deformation such as element bow and diametral creep. The bundle geometry is based on the post-irradiation examination (PIE) data of a single bundle from the Bruce B Nuclear Generating Station, Bruce B bundle G85159W, which was irradiated for more than two years in the core during reactor commissioning. The subchannel code ASSERT-PV IST is used to assess changes in CHF and dryout power due to bundle deformation, compared to the reference, undeformed bundle.

1. INTRODUCTION

Dimensional changes of a fuel bundle may reduce the bundle performance limit and operating margin. One of the limiting factors is a potentially lowered critical heat flux (CHF) margin due to bundle geometry changes during the irradiation. It is therefore essential to assess the effect of bundle deformation on CHF margins. No subchannel thermalhydraulic analysis was previously reported on the effect on CHF of bundle deformation such as that observed in the extended burnup Bruce B bundle G85159W. The effect is assessed with the subchannel code ASSERT-PV IST in the present work.

1.1 Background of Bundle G85159W and post-irradiation examination (PIE) measurement

Bundle G85159W was part of the initial fuel load for Bruce-B unit 7 and was manually loaded into position 8 of Channel H07 on 1984 October 9. Position 8 is the fifth bundle position from the coolant inlet end of the channel. After residing in the core during reactor commissioning, it was irradiated for more than two years (from 1986 February 28 to 1988 May 29). The irradiation of this bundle involved about 13 power cycles of the reactor with power reductions exceeding 10% full power. The bundle achieved a high burnup of 492 MWh/kgU.

The geometric change of the high burnup Bruce bundle was estimated through post-irradiation examination (PIE). The inner 19 elements were profiled only after the bundle was carefully disassembled. The outer 18 elements were profiled before and after the disassembly for comparison. Most element profiles remained unchanged, indicating that the method of disassembly did not introduce significant permanent distortions to the elements and that there was no significant elastic component of strain of the irradiated elements. Furthermore, the worn surfaces of the bearing pads of the bottom elements fell on a straight line indicating that all 3 bearing pads of each bottom element were in contact with the pressure tube, as expected, and that the measured profiles were close to that expected in-reactor during normal operating conditions. The PIE measurements included profiles and diameters of all fuel elements and profiles and tilt of both endplates. Most measurements, including element bow, endplate distortion, bearing- and spacer-pad wears, were found to be generally within the typical range observed for CANDU power-reactor fuels irradiated to ~200 MWh/kgU. Any elastic deformation that occurs in reactor during refuelling or hypothetical accidents is not measured during PIE. This assessment is based on permanent deformation only.

1.2 Mapping of the PIE data

PIE measurements were analyzed using a spreadsheet program called EXLACS (EXCEL Looking A Lot like CADDS) to assess the deformation of endplates and elements. EXLACS calculates the cross-sectional geometry of an irradiated fuel bundle using the fuel element profilometry data collected during PIE. It converts the PIE profile measurements into a three-dimensional pattern of bundle deformation by generating eight two-dimensional, cross-sectional maps of distributions of element bow and element diametral creep. The results revealed plastic deformation of the bundle, such as inward bow of top elements as well as sagging or “settling” of the bundle toward the pressure-tube (PT). The deformation is summarized as follows:

(a) top-element inward bow of up to 1.1 mm (at the axial mid-plane),
(b) element diametral creep of up to 0.1 mm,
(c) endplate tilt of up to 0.2^{o},
(d) endplate droop of about 0.1-0.3 mm, and
(e) considerable spacer fretting near the top of the bundle.

1.3 CHF Analysis Tool – ASSERT-PV IST

ASSERT-PV is a subchannel thermalhydraulic code capable of predicting the detailed subchannel-level fluid flow and heat transfer in CANDU[1] reactor fuel bundles. It is

[1] CANDU® is a registered trademark of Atomic Energy of Canada Limited (AECL)

based on the subchannel concept widely used for fuel-bundle thermalhydraulic analysis, where the fuel bundle is divided into smaller sections called subchannels. Equations of mass, momentum and energy are solved for each subchannel while taking into account the possible inter-subchannel interactions. ASSERT-PV computes flow and phase distributions in subchannels of a CANDU fuel bundle, and provides a detailed prediction of CHF, post-dryout (PDO) heat transfer and fuel sheath temperature distributions throughout the fuel bundle [1-2].

Since ASSERT-PV computes detailed flow and phase distributions, and predicts CHF and flow distribution in subchannels of nominal or deformed CANDU fuel bundles in uncrept and crept fuel channels, it is the ideal tool for performing thermalhydraulic assessment of the impact of the bundle deformation on CHF and hence dryout power for the extended burnup Bruce bundle G85159W. The latest version of the code, ASSERT-PV IST V3R1, is used in the present thermalhydraulic analysis. Validation of ASSERT-PV for dryout power and pressure drop with reference undeformed bundles [2] is considered applicable to bundles with small deformations.

2. MODELLING AND METHODOLOGY

2.1 Forms of Bundle Deformation

The impact of bundle deformation on the ASSERT-PV model is discussed below.

<u>(a) Element bow</u> Since the fuel elements are constrained at the endplates, they tend to bend or bow in-reactor. The non-linearity of the element bow results in changes in subchannel flow area, which in turn can affect CHF and dryout power through changes in flow distribution. This form of deformation is important because changes in flow area may significantly affect CHF and dryout power. The element bow is modelled by ASSERT-PV through input of PIE measurements.

<u>(b) Element diametral creep</u> Element diametral creep could result in changes in subchannel flow area. However, a diametral creep of up to (and generally much smaller than) 0.1 mm is small, and is expected to have much less impact on the subchannel flow area and the flow distribution than element bow, which is one order of magnitude larger. The element diametral creep is modelled by ASSERT-PV through input of PIE measurement data.

<u>(c) Endplate tilt</u> The downstream end of the fuel string is normally supported on a vertical plane defined by the latch fingers in Bruce. The bottom of the fuel string is supported by the pressure tube which sags under the influence of irradiation. The net result is that the bundles become permanently parallelogrammed, resulting in endplates that are not at right angles with the bundle centreline. This bundle distortion is called endplate tilt. Endplate tilt of up to 0.2° is too small to have any meaningful effect on subchannel flows. This is because this deformation results in maximum local displacements of only 0.2 mm in the axial/flow direction and 0.001 mm in the cross-

sectional plane, which should be compared, respectively, to the bundle length of about 500 mm and to the PT diameter of about 100 mm. The endplate tilt is therefore not considered in the ASSERT-PV assessment.

(d) Endplate droop The weight of the fuel bundle on the pressure tube is supported by a few end bearing pads located on bottom fuel elements. Since there is very little support of the bundle at the midplane, most of the bundle weight is transferred through the endplates to these bottom elements, causing the bundle endplates to droop downward. This lowers the bundle centreline which is already offset relative to the pressure tube. The elevation (or droop) of the endplate is also affected by the material loss due to sliding wear on the bottom bearing pads. The net result is that due to the endplate droop effect, the bundle centreline is lowered by up to 0.3 mm and possibly tilted if the degree of endplate droop is different for the two endplates. Since ASSERT-PV can only model a bundle with centreline being parallel to that of the PT, a sensitivity study on the effect of endplate droop is performed, in which the bundle centreline is shifted downward by 0.3 mm relative to that without the endplate droop, minimizing the bottom subchannels between the outer elements and PT to maximize the endplate droop effect.

(e) Spacer fretting Considerable fretting was observed on the spacers of the top elements with estimated wear depth up to 0.2 mm, and up to 0.1 mm at other locations. The measured profiles of the elements confirmed that the gaps at those locations were reduced. The reduced gap between elements reduces the subchannel flow areas, which was taken into account through modelling of the PIE element bow. Since the fretting only occurs on the small area of contact between mating spacers, the spacer height is not significantly affected. Therefore, the effect of spacer fretting on local flow resistance, i.e., the form loss/drag, is expected to be minimal, and the effect is not considered in the ASSERT-PV assessment.

2.2 ASSERT-PV Modelling of the Bundle Geometry and Phenomena

Except for the element bow and element diametral creep, all other geometric models and phenomenon modeling options, such as that for the CHF model, are the same as used in the validation exercise of ASSERT-PV. This is because the validation exercise dealt with the details of a standard Bruce bundle, including endplates, bearing pads and spacers, and the models were validated against the Stern Laboratories' pressure drop and CHF experiments [3] that covered conditions representative of normal operations and LOF, LOR, and SBLOCA accident scenarios.

The 37-element bundles modeled in the present work are typical Bruce bundles, each having two endplates, five planes of bearing pads and one plane of spacer pads, which are modeled only for their resistance to the flow, as local drag force, and their enhancement of CHF, though empirical models. There are 12 identical bundles in the bundle string, with each bundle being divided into 12 grids or control volumes along the axial direction. The bundles are assumed fully aligned at the boundaries of each bundle. Analysis with ASSERT-PV is limited to bundle strings with fully aligned bundles.

With the fuel channel and bundle geometry data specified in the ASSERT-PV input file, the built-in geometric pre-processor in ASSERT-PV computes the subchannel geometry, including the subchannel flow areas, heated and wetted perimeters, the inter-subchannel gap widths, and the subchannel centroid-to-centroid lengths and angles. A subchannel is defined as the coolant flow area bounded by the rod surfaces and imaginary lines joining adjacent rod centres. The subchannel discretization is shown in Figure 1(a) for a nominal 37-element bundle in an uncrept channel.

ASSERT-PV modeling of element bow and diametral creep is through input-data tables in the ASSERT-PV input file, in which element bow (displacement) and diametral change are specified at axial locations for each of the 37 elements. Data from the EXLACS spreadsheet are available at eight axial positions for each of the 37 elements. These axial positions are shown in Figure 2; and a cross-sectional view generated by ASSERT-PV is shown in Figure 1(b) for an axial location near the axial mid-plane of the bundle, where the deformation is generally larger than at locations near the bundle ends where elements are constrained by bundle endplates. Note that the bundle is rotated clockwise by 70 degrees from the nominal position shown in Figure 1(a), based on the PIE measurement of bearing pad wear that suggested that element #25 was the bottom element during irradiation.

(a) (b)

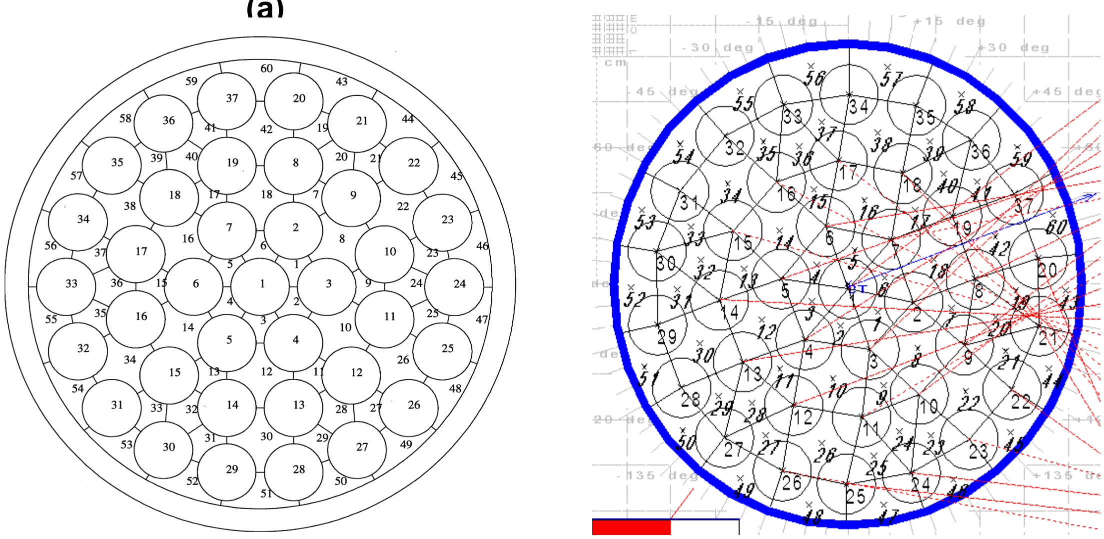

Figure 1 ASSERT-PV model of 37-element CANDU bundle: (a) nominal bundle; (b) cross-sectional view of Bundle G85159W in uncrept PT, 290 mm from the upstream endplate.

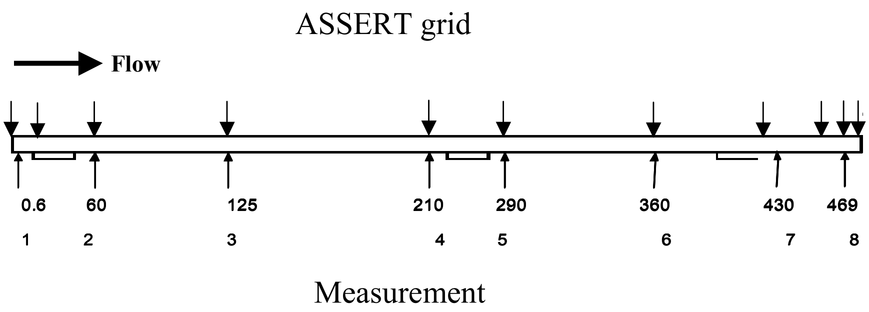

Figure 2 Axial locations of PIE measurement and ASSERT-PV nodal points.

Figure 3 shows the axial variations in inside diameter of crept PTs in simulation cases. These axial diameter variations are also specified in the ASSERT-PV input file, together with other channel and bundle geometries. They are typical PT creep profiles used in assessing the effect of PT creep in the validation of ASSERT-PV and in the Stern Laboratories' experiments. Also shown in Figure 3 is the axial power distribution; the downstream-skewed cosine-shaped profile is the same as used in Stern Laboratories' experiments and the validation exercises.

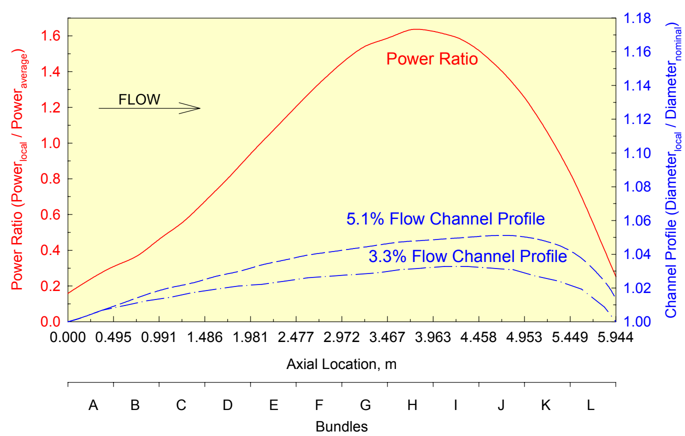

Figure 3 Typical Axial Power Profile and Flow Channel Variations (Maximum PT Diametral Creep of 3.3% and 5.1%).

The ideal axial nodalization would be to match computational nodes to the measurement locations, to avoid any interpolation that would introduce added uncertainty. This is not always possible with a limited number of nodes because numerical accuracy and stability requires that neighbouring axial zones should not be too different in size. The ASSERT-PV nodal grid is also shown in Figure 2.

2.3 Adjustment of Gap Width between Intermediate Elements 10 and 11

From Figure 1(b), a substantial decrease in gap size can be seen for the gap between intermediate elements #10 and #11. The gap width near the mid-plane of the bundle is about 0.8 mm if calculated from the original PIE data of element bow, which is possible only with severe spacer fretting of the interfering spacers resulting in a total wear depth of 0.5 mm. However, the PIE estimate indicates that one of the two interfering spacers had a wear depth of about 0.1 mm and the other about 0.05 mm. Therefore, it is reasonable to assume that the gap width in question should not be smaller than about 1.1 mm, and that the associated elements were less bowed when “in bundle” (with elastic deformation) than was indicated by the PIE data from “loose-element” measurement (the two elements bowed roughly towards each other). Based on this reasoning, the element bow of element #11, which has a much larger bow than element #10, is adjusted to result in a minimum gap width of about 1.1 mm.

2.4 Simulation Runs

ASSERT-PV simulations are performed for three basic cases:

(1) A reference bundle string with no deformed bundles;
(2) A bundle string with three deformed bundles placed at #9-#11 from the channel inlet (the three bundles where CHF is most likely to occur).
(3) A bundle string with all 12 bundles deformed.

To facilitate comparison with the reference bundle string, all deformed bundles are assumed identical (based on bundle G85159W), regardless of axially varying power and PT creep profiles.

The effect of these deformations is assessed for the following matrix of operating conditions and PT creep profiles:

- Pressure: 9 and 11 MPa
- Flow rate: 14 and 21 kg/s
- Inlet temperature: 240 and 265 °C
- PT creep: 0%, 3.3% and 5.1% (maximum)

The total number of simulation runs is thus 72.

3. RESULTS AND DISCUSSION

3.1 Channel Dryout Power

The channel dryout power, or onset-of-dryout power (ODP), is obtained through a built-in iteration process that iterates on the average channel heat flux until CHF is predicted to occur. Figure 4 shows results for channel dryout power as relative difference between the dryout power of a deformed bundle string and that of the reference bundle string; the relative difference is plotted against the dryout power of the reference bundle string. It should be noted that the dryout power itself is not a controlled parameter in the present simulation; using it as a coordinate of this figure is simply to spread the data points in the figure for an easier comparison. For both the case of three deformed bundles and the case of all bundles deformed, the relative difference or percentage change is positive, indicating an increased dryout power due to the deformation of bundle G85159W. From this figure, it can also be found that the case of three deformed bundles generally results in a slightly higher dryout power than does the case of all bundles deformed; and the effect of bundle deformation is stronger for the 9 MPa than for the 11 MPa cases. The differences are, however, not significant from an engineering point of view. For all simulated cases, the average of relative differences is 3.4%, with the minimum being 1.0% and the maximum being 5.7%.

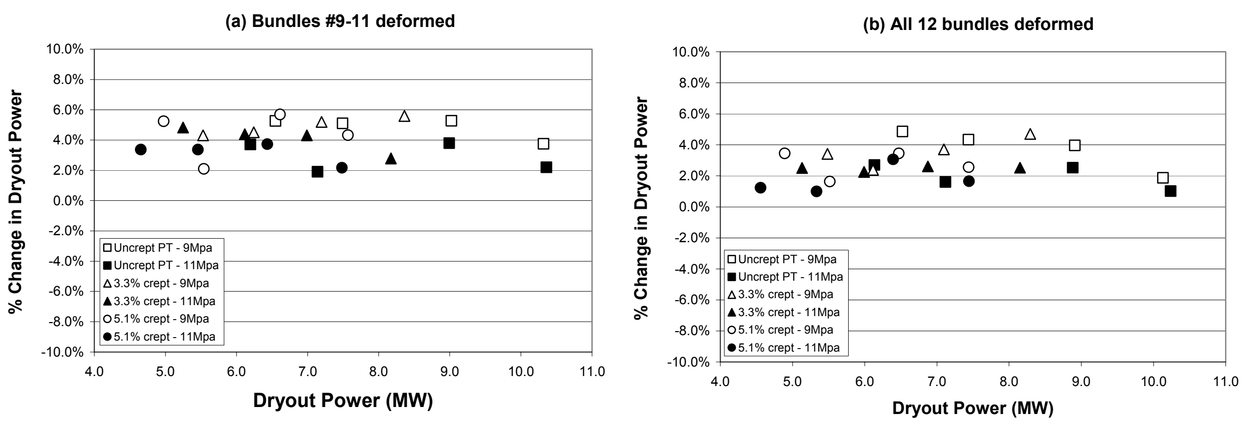

Figure 4 Percentage change in dryout power due to bundle deformation: (a): Bundles #9-11 deformed; (b): All bundles deformed.

3.2 Effect of Bundle Deformation on Flow Distribution and CHF

Although upstream history may play a considerable role in CHF under certain conditions, here CHF appears to be a local phenomenon. Detailed examination of the simulation results shows that for a reference, undeformed bundle, CHF occurs mostly at or near the downstream end of elements #7 or #6, facing mostly the uppermost inner subchannel #5 or sometimes the neighbouring subchannel #4 (see Figure 1(b)). It was found that the local flow/void fraction change at locations where CHF is likely to occur has a direct impact on CHF and dryout power.

Figure 5 shows the axial variation in subchannel area due to the bundle deformation, for top inner subchannels #5 and #4, where CHF usually occurs (on elements #7, 6 or 5). The subchannel flow areas of the deformed bundle in a nominal PT are compared with those of a reference, undeformed bundle. For subchannel #5, the decrease in flow area is moderate near the bundle mid-plane, and the flow area actually increased slightly, about 1-2%, near the downstream end of the bundle where CHF is likely to occur for a nominal bundle. For subchannel #4, the increase in flow area is observed throughout the bundle length. Change in flow rate and void fraction may result not only from flow area change but also from change in flow distribution due to two-phase flow mixing enhanced by the flow area change. For example, if there are subchannels with reduced subchannel flow area, void generation in these subchannels could accelerate, resulting in a decrease in flow rate by much more than the percentage with which the flow area is decreased, and vice versa. Furthermore, the void fraction change in one subchannel is affected also by flow changes in neighbouring subchannels since the subchannels are inter-connected with two-phase-flow mixing across the boundaries.

Figure 6 shows, as an example, the axial void fraction distribution for the “hot” subchannels #5 and #4, in which the void fraction with the deformed bundle is seen decreased for both subchannels, compared to that with the reference bundle, suggesting an increased CHF and dryout power.

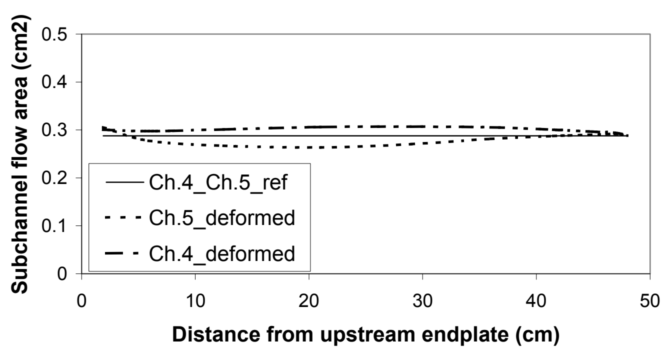

Figure 5 Change in subchannel flow area due to bundle deformation, for inner subchannels #4 and #5.

3.3 Results of a Sensitivity Study of the Effect of Endplate Droop

As described in Section 2.1, in this sensitivity study, the bundle centreline is lowered by 0.3 mm, relative to the case without endplate droop, towards the bottom of the PT to maximize the effect of the endplate droop. This results in an offset of 1.0 mm between the bundle and the PT centrelines. The resulting change in dryout power, compared to the base case, is very small, with the average difference, standard deviation, and maximum difference being -0.0%, 0.2% and -0.5%, respectively. The result indicates that the effect on dryout power of the endplate droop is insignificant.

4. CONCLUDING REMARKS

- Relative to the reference, undeformed bundle string, the predicted dryout power of the deformed bundle string, for the flow conditions and geometry given in Section 2.4, ranges from a 1.0% to a 5.7% increase with an average of a 3.4% increase.

- A sensitivity study was performed in which the bundle centreline was shifted downward by 0.3 mm to maximize the effect of the endplate droop. The resulting change in dryout power, relative to the case without the endplate droop, was predicted to be very small, with the maximum difference being a 0.5% decrease.

- The increase in dryout power may be due to the particular deformation of G85159W that resulted in increased flow and decreased void fraction in the “hot” subchannel on top of the centre element, especially near the downstream end of the bundle, where CHF is most likely to occur for a reference buddle. Analyses on other similarly deformed bundles are under way for further investigation.

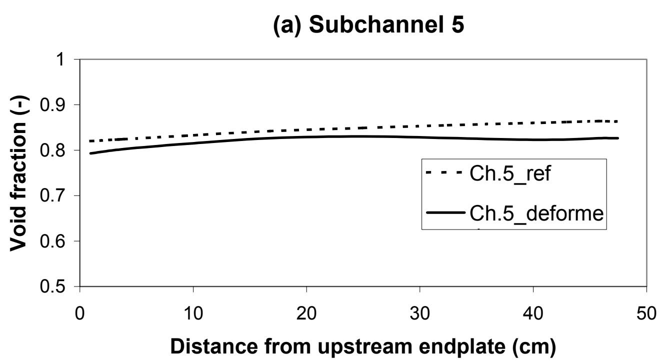

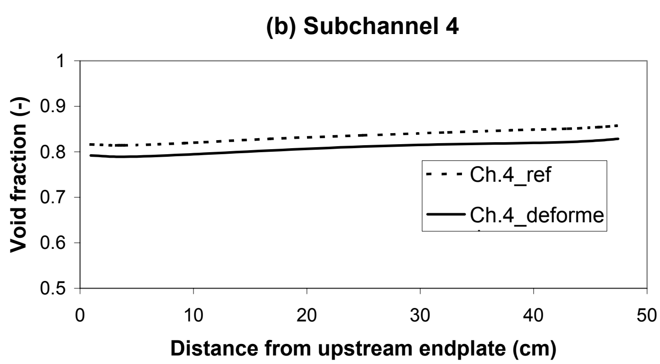

Figure 6 Effect of bundle deformation on void fraction in subchannels #5 and #4 with pressure of 9 MPa, inlet temperature of 265°C, flow rate of 14 kg/s, dryout power for the reference case, and uncrept PT.

ACKNOWLEDGEMENT

The work reported in this paper was funded by CANDU Owners Group (COG), Work Package No. 22220 in the Fuel Normal Operating Conditions Working Group.

REFERENCES

1. Carver, M.B., Kiteley, J.C., Tahir, A., Banas, A.O. and Rowe, D.S., “Simulation of flow and phase distribution in vertical and horizontal bundles using the ASSERT subchannel code,” Nuclear Engineering and Design 122, 413-424, 1990.
2. Rao, Y.F. and Hammouda, N., “Recent Development in ASSERT-PV Code for Subchannel Thermalhydraulics,” 8th CNS International Conference on CANDU Fuel, Honey Harbor, Ontario, Sep 21-24, 2003.
3. Leung, L.K.H., Groeneveld, D.C. and Hotte, G., “Prediction Methods to Account for the Effect of Pressure-Tube Diametral Creep on Critical Heat Flux and Pressure Drop for a 37-Element Bundle String”, 19th CNS Simulation Symposium, Hamilton, Ontario, October 16-17, 1996.